



## Experimental Investigation on Effects of Trapezoidal Ribs on Heat Transfer Enhancement with Electrohydrodynamics Active Method into Duct

A. Alami-nia

Department of Mechanical Engineering, Azarbaijan Shahid Madani University, Tabriz, 53751-71379, Iran

**ABSTRACT:** In this work, the heat transfer enhancement of trapezoidal ribs is investigated. Cooling of the three trapezoidal ribs has been achieved with electrohydrodynamics active method by experimental apparatus. The hydrodynamic and heat transfer behavior of air flow was studied by electrohydrodynamics active method. The aim of the present work is heat transfer enhancement with low pressure loss. In active method, two arrangements of wire electrodes have been applied. The results show that in the same Reynolds numbers and voltages of wire electrodes, the heat transfer was increased in arrangement 1 than arrangement 2. Density of electric charge around wire electrodes in arrangement 1 is higher than in arrangement 2. Therefore, arrangement 1 is better than arrangement 2. Arrangements 1 and 2 are different with the position of wire electrodes. With attention to results the power of corona wind in low Reynolds flows is higher than in high Reynolds flows, signifying that the corona wind in low Reynolds numbers is better than in high Reynolds numbers. In the same Reynolds numbers and voltages of wires, the average performance evaluation criteria were increased in arrangement 2 than arrangement 1.

### Review History:

Received: Aug. 14, 2019

Revised: Nov. 16, 2019

Accepted: Dec. 09, 2019

Available Online: Feb. 18, 2020

### Keywords:

Enhancement

Convection

Electrohydrodynamics

Ribs

Corona wind

### 1- Introduction

Due to using various elements in local heat sources and boards and size reduction, the cooling element has become a vital part of the system. The active method with application of corona wind is a well-known method for heat transfer enhancement. The present work applies Electrohydrodynamics (EHD) active methods for heat transfer enhancement. The EHD active cooling system is a new cooling method that has been developed in our fluid mechanics and heat transfer laboratory.

Alami nia and Esmaeilzadeh [1], studied the heat transfer enhancement of rectangular ribs located in a rectangular duct experimentally. In this work, the behavior of air flow was studied by passive, active and compound methods. The results showed that the heat transfer enhancement was increased for the compound method in low Reynolds numbers. Alami nia and Esmaeilzadeh [2, 3], investigated the numerical study on the heat transfer enhancement of rectangular ribs located in a 3D duct has been achieved. The results showed that the heat transfer enhancement was increased for passive method in high Reynolds numbers.

Alami nia et al. [4, 5, 6], studied the heat transfer enhancement of flush-mounted ribbons inserted in a rectangular duct. In this work, the behavior of air flow was studied by active EHD method. The results showed that the heat transfer enhancement was increased for active method

in low Reynolds numbers.

Peng et al. [7] investigated the numerical simulation of heat transfer enhancement in a rectangular channel by electrohydrodynamics. In this study, the effects of longitudinal position have been achieved for single electrode, longitudinal arrangement for multiple electrodes, and electrode number with an optimal longitudinal arrangement. A factor defined as the ratio of average heat transfer coefficient with EHD to that without EHD is used to evaluate the level of EHD-induced heat transfer augmentation. The results showed that as the electrode number exceeds a certain value, with the optimal electrode arrangement reaches a plateau; further increasing the electrode number only increases the power consumption but has no contribution to the heat transfer enhancement. The results indicated here are limited to the geometry and parameter range used in this study.

Sheu et al. [8] investigated the effect of oscillatory EHD on the heat transfer performance of a flat plate. A needle-type electrode with positive polarity was used to generate ionic wind with applied voltage ranging from 4 to 9.5 kV. The wave forms of the input voltage were either steady or stepped and the frequency ranges from 0.5 to 2 Hz with the separation distance between the electrode and the test plate being 5 and 15 mm, respectively. It was found that at the same applied voltage, the heat transfer performance subject to the oscillatory EHD was always inferior to that of the steady EHD for all frequencies. A parabolic dependence of the ionic current

\*Corresponding author's email: amin.alam@azaruniv.ac.ir



Copyrights for this article are retained by the author(s) with publishing rights granted to Amirkabir University Press. The content of this article is subject to the terms and conditions of the Creative Commons Attribution 4.0 International (CC-BY-NC 4.0) License. For more information, please visit <https://www.creativecommons.org/licenses/by-nc/4.0/legalcode>.

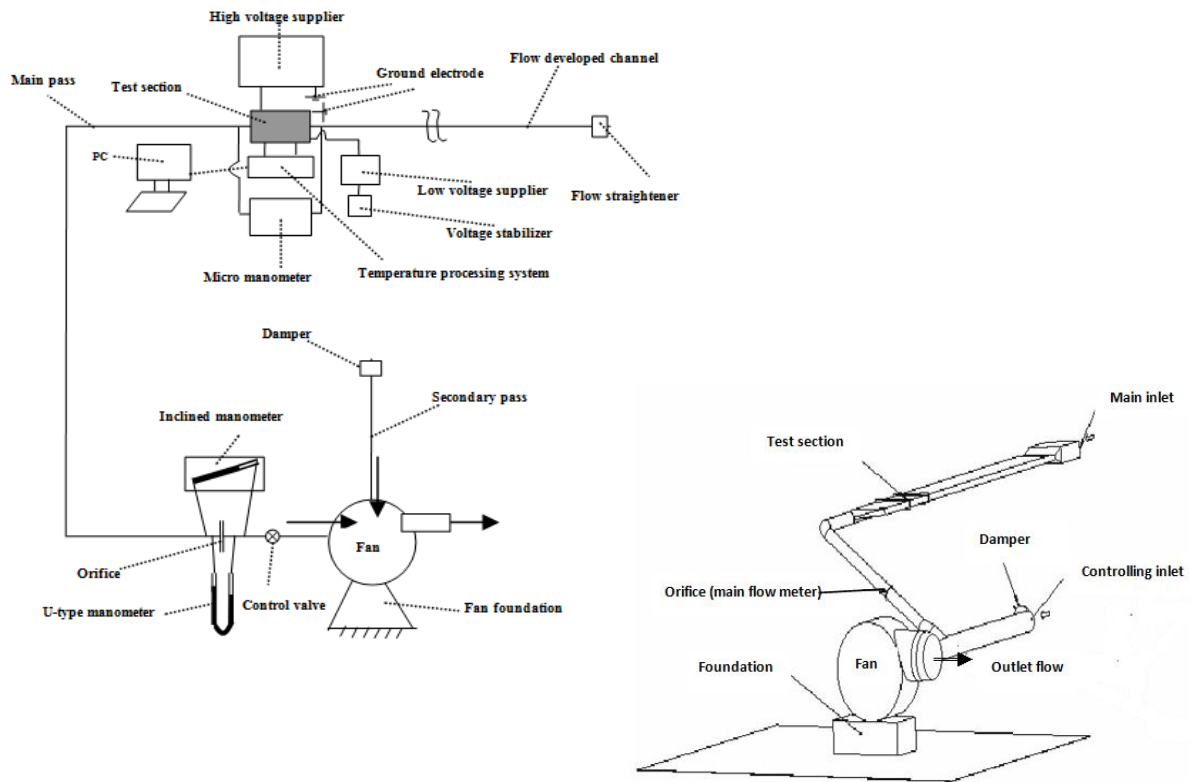


Fig. 1. The schematic and the layout of the main apparatus

with supplied voltage was seen under steady EHD operation. However, the ionic current versus supplied voltage showed a rather linear dependence pertaining to the oscillatory EHD. For a smaller separation distance of 5 mm, the heat transfer performance for  $f = 0.5$  Hz was slightly higher than that of  $f = 2$  Hz. However, the trend has reversed when the separation distance increased to 15 mm.

Deylami et al. [9] investigated the numerical study of forced convection heat transfer enhancement with EHD technique of turbulent flow inside a smooth. A two dimensional numerical approach has been chosen to evaluate the local and average heat transfer coefficient. In addition, the swirling flow pattern in the presence of an electric field has been studied. To achieve higher enhancement while using multiple electrodes, a variety of electrode arrangements have been examined for specified values of Reynolds number, applied voltage, and wire radius. The results demonstrate that different electrode arrangements cause a significant improvement of heat transfer coefficient.

Fujishima et al. [10] studied the flow behavior of the main flow and the secondary flow in wire-duct electrostatic precipitator. They extended to incorporate alternately oriented point corona on wire-plate type electrodes.

Ohadi et al. [11] studied the heat transfer enhancement in pipe flow with wire-plate electrodes. The results showed that the heat transfer enhancement was increased for the two-wire electrode than the single wire electrode.

## 2- Experimental Investigation

For the design of the test section, the following conditions have been achieved:

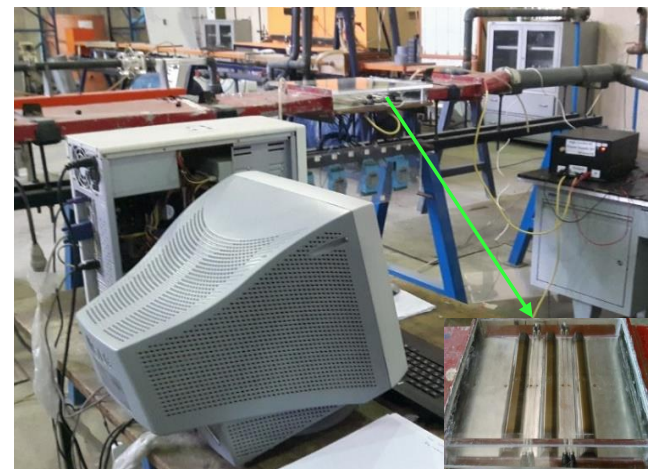


Fig. 2. Photo of the main setup

A fully developed air flow should be supplied before the flow enters the test section. The apparatus is designed to flow with low and high values of Reynolds numbers. Reynolds number ( $Re_{D_h} = vD_h/\nu$ ) has been based on hydraulic diameter of channel ( $D_h = \frac{2WH}{W+H}$ ) under laminar and turbulent ( $Re_{D_h} = 500, 2000$  and  $4500$ ) regimes. The flow was 3D, steady, viscous and incompressible with very small Mach numbers,  $M < 0.3$ .

Fig. 1 shows the schematic and the layout of the main experimental apparatus. A centrifugal fan with fixed rotation speed was used to produce the air flow. Fig. 2 shows the photo of the main experimental apparatus.

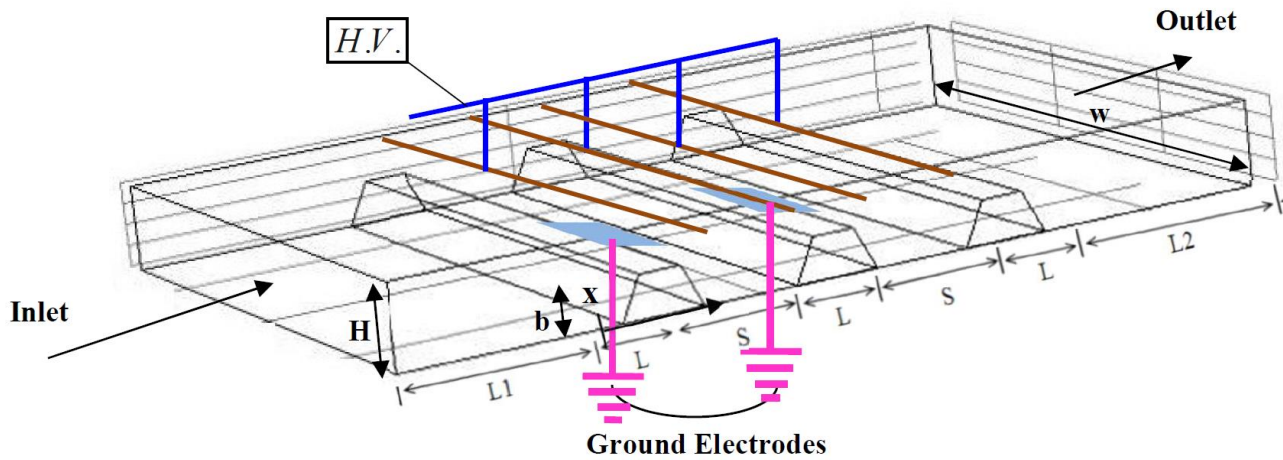


Fig. 3. Schematic and geometry of the test section

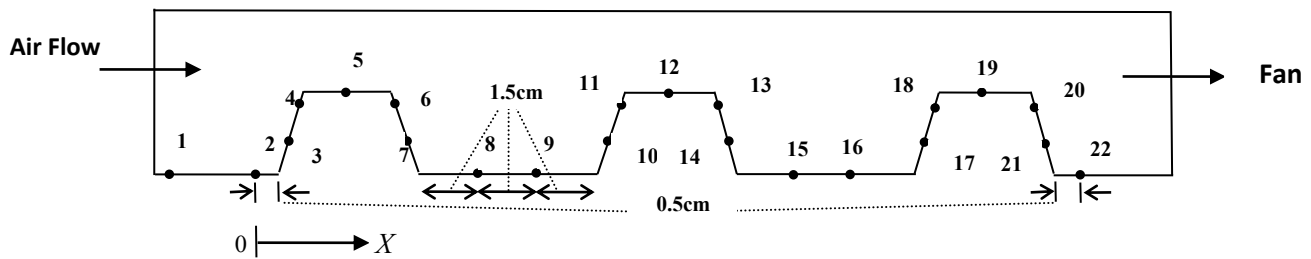


Fig. 4. The thermocouples arrangement

The test section was designed to be a channel with 40cm length,  $H=4\text{cm}$  height, and  $W=30\text{cm}$  width as shown in Fig. 3. The hydraulic diameter of the test section was 7.06cm. The geometry of trapezoidal ribs arrangements as illustrated in Fig. 3 are:

$$L_1 = L_2 = 107.5\text{mm}; L = 40\text{mm}; S = 45\text{mm}; b = 20\text{mm}; H = 40\text{mm} .$$

The flow rate was measured by orifice meter under the France standard NF X10-102 [12]. In the test section, the ribs were electrically heated with constant heat flux. The trapezoidal ribs had 3cm in width, 30cm in length, and 3cm in axial spacing between them. 22 thermocouples were used for measuring the temperature of the bottom channel wall and the ribs surface in the central direction of flow. The type of thermocouples is T-type with Cu-Constantan ( $C/C_T$ ). The geometric layout of thermocouples is shown in Fig. 4.

For the measure of temperature, the ADAM digital system was used. High voltage is applied using a high voltage supplier for the EHD wire-plate active method. The high voltage supplier generated voltages up to 40kV between the wire and ground electrodes. The arrangement of electrodes with their geometric coding values is illustrated in Fig. 5.

The purpose of this work is to study the heat transfer enhancement for 3D traverse trapezoidal ribs located at the floor of the channel.

Three parameters characterize the laminar air flow with heat transfer:

- 1) Rate of heat transfer enhancement  $E_t$ ,

$$E_t = \frac{h}{h_s} = \frac{(T_w - T_{ref})_s}{(T_w - T_{ref})} \quad \text{with} \quad h = \frac{q''_{rib}}{T_w - T_{ref}} \quad (1)$$

- 2) consumed power ratio  $E_{lost}$ ,

$$E_{lost} = \frac{\Delta P}{\Delta P_s} \quad (2)$$

- and 3) performance evaluation criteria (PEC)  $\eta_e$ ,

$$\eta_e(PEC) = \frac{E_t}{E_{lost}} \quad (3)$$

In the sequence of Eqs. (1) to (3),  $q''_{rib}$  is the constant heat flux from trapezoidal ribs to fluid flow,  $h$  is the local heat transfer coefficient,  $T_{ref}$  is the reference temperature (inlet

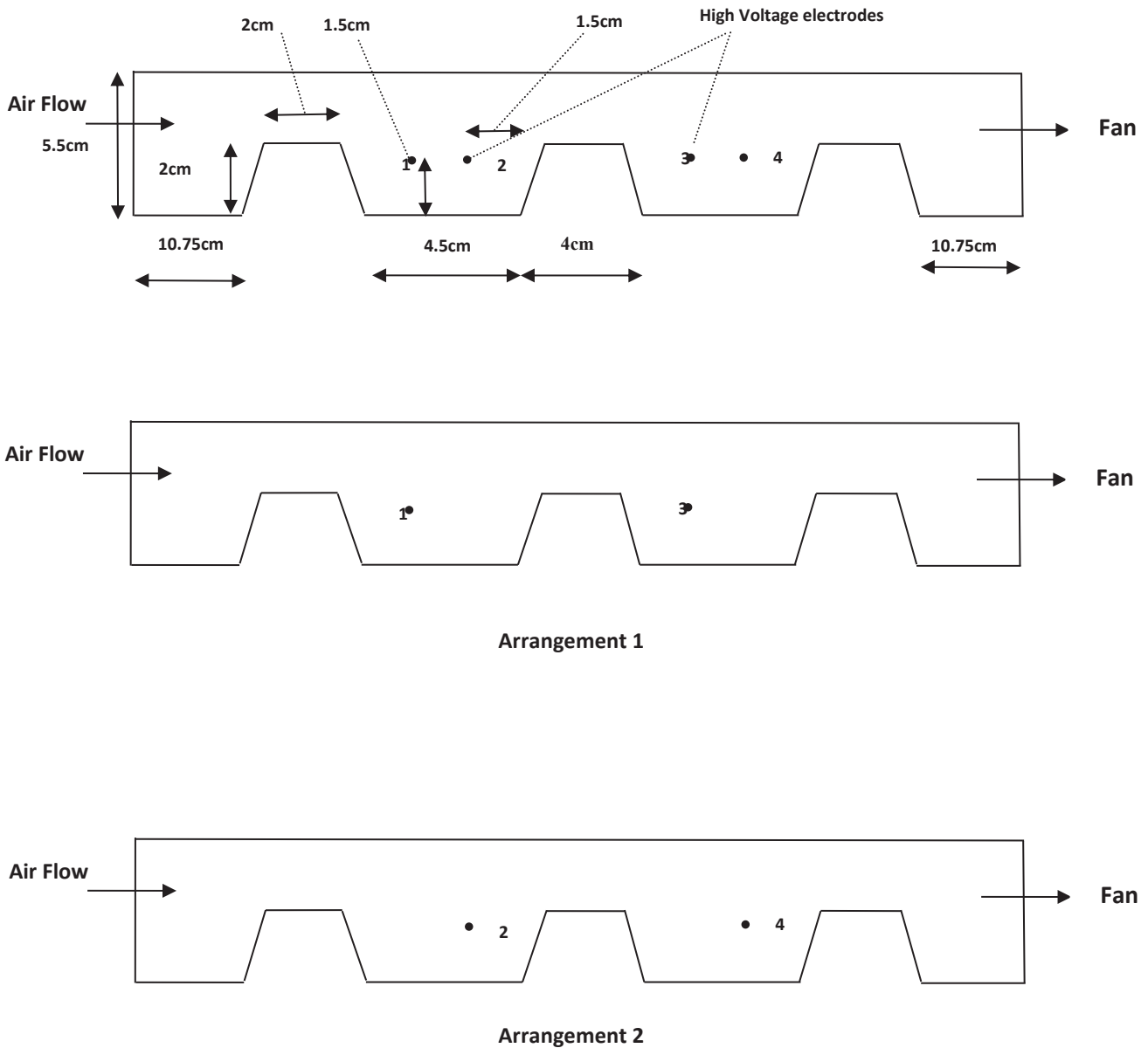


Fig. 5. Arrangements of wire electrodes

temperature to the test section),  $T_w$  is the temperature of the surface of trapezoidal ribs on the floor of the test section, including the surface of trapezoidal ribs and spacing of them,  $\Delta P$  is the pressure loss, and subscript s denotes the plain case without enhancement intervention.  $Re_{D_h}$  is Reynolds number based on the hydraulic diameter of the channel,  $N_{EHD}$  is EHD number.  $N_{EHD}$  is defined as:

$$N_{EHD} = \frac{\rho_e E_0^2 L^2}{\rho_f \nu_f^2} = \frac{b E_0 L}{\nu_f} = \frac{u_i L}{\nu_f} \quad (4)$$

This parameter is similar to the  $Re_{D_h}$  number based on the velocity of electric ions  $u_i$  and with the assumption of similar density for ions and neutral fluid particles. In Eq. (4),  $\rho_e$  is density of electric charge,  $\rho_f$  is density of fluid,  $E_0$  is electric field,  $b$  is mobility of ions, and  $\nu_f$  is the kinematics viscosity

of fluid.  $u_i$  is defined as:

$$u_i = \frac{I_0}{q_{e0}} \quad (5)$$

In this equation,  $I_0$  is the electric current of corona wind,  $q_{e0}$  is the electric charge of one electron, which is  $1.602 \times 10^{-19}$  Coulomb.  $L$  is the characteristic length and defined as [13]:

$$L = D_h \times \alpha \times \frac{C}{H} \times \ln\left(\frac{r_{eff}}{r}\right) \quad (6)$$

where:  $\alpha$  is the view angle between wire and ground electrodes ( $\alpha = 1$  for the case of one wire electrode between two ground electrodes and  $\alpha = 0.5$  for the case of one wire and one ground electrode).  $C/H$  is the ratio of space of wire

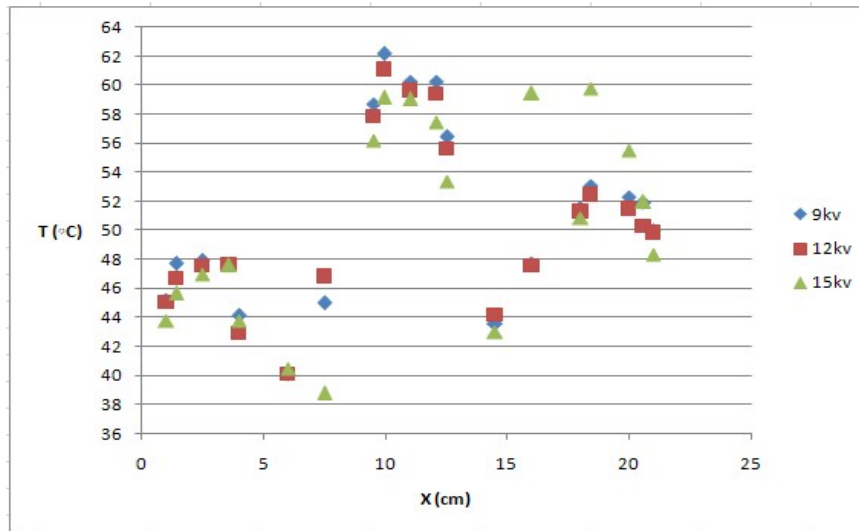


Fig. 6. Distribution of wall temperature on rib's surface direction for arrangement 1 and  $Re_{D_h} = 0$

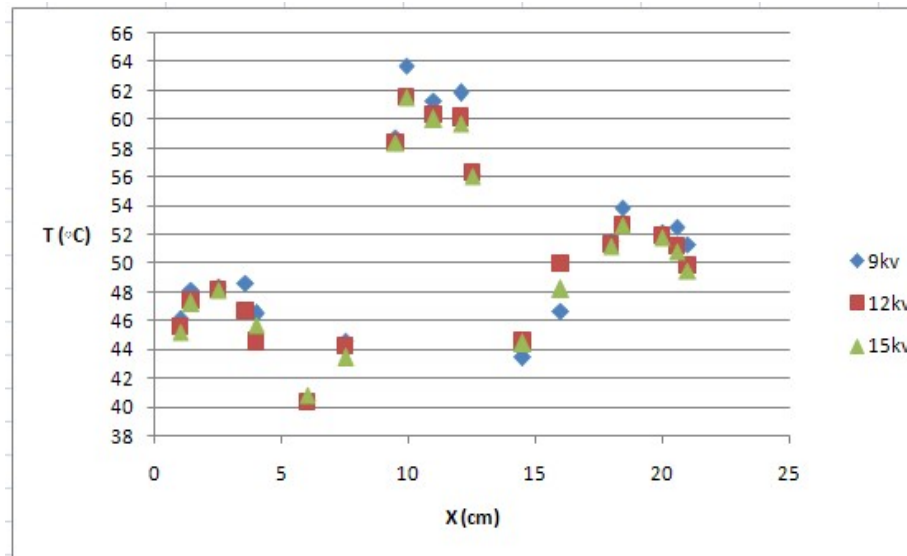


Fig. 7. Distribution of wall temperature on rib's surface direction for arrangement 2 and  $Re_{D_h} = 0$

and ground electrodes to channel height.  $r_{eff}/r$  is the ratio of effective radius of wire and ground electrodes to the radius of wire electrode and  $r_{eff}$  is defined as  $r_{eff} = 4C/\pi$ , where C is the distance between wire and ground electrodes.

### 3- Results and Discussion

Figs. 6 and 7 show the distribution of wall temperature for the EHD case for arrangements 1, 2, and  $Re_{D_h} = 0$ .

In Figs. 8 and 9, the rate of heat transfer enhancement for the EHD case (arrangements 1, 2,  $Re_{D_h} = 0$ ) is shown. The effect of voltage on heat transfer enhancement is shown in the Figures. The impact of voltage and arrangement of wire electrodes has been shown in these Figures. The local and average heat transfer enhancement for voltage 15kV and arrangement 1 is higher than others. The density of electric

charge around of wire electrode in arrangement 1 is higher than in arrangement 2. Therefore, arrangement 1 is better than arrangement 2.

In Figs. 10 to 13, the distribution of wall temperature for the EHD case (arrangements 1, 2,  $Re_{D_h} = 500$  and 4500) is shown.

In Figs. 14 to 17, the rate of heat transfer enhancement for the EHD case (arrangements 1, 2,  $Re_{D_h} = 500$  and 4500) is shown. The impact of voltage and arrangement of wire electrodes on the heat transfer enhancement has been shown in the Figures. The local heat transfer enhancement for voltage 15 kV and arrangement 1 is higher than others. The density of electric charge around of wire electrode in arrangement 1 is higher than that in arrangement 2. Therefore, arrangement 1 is better than arrangement 2. For high Reynolds numbers, the power of the main flow is higher than the power of corona wind

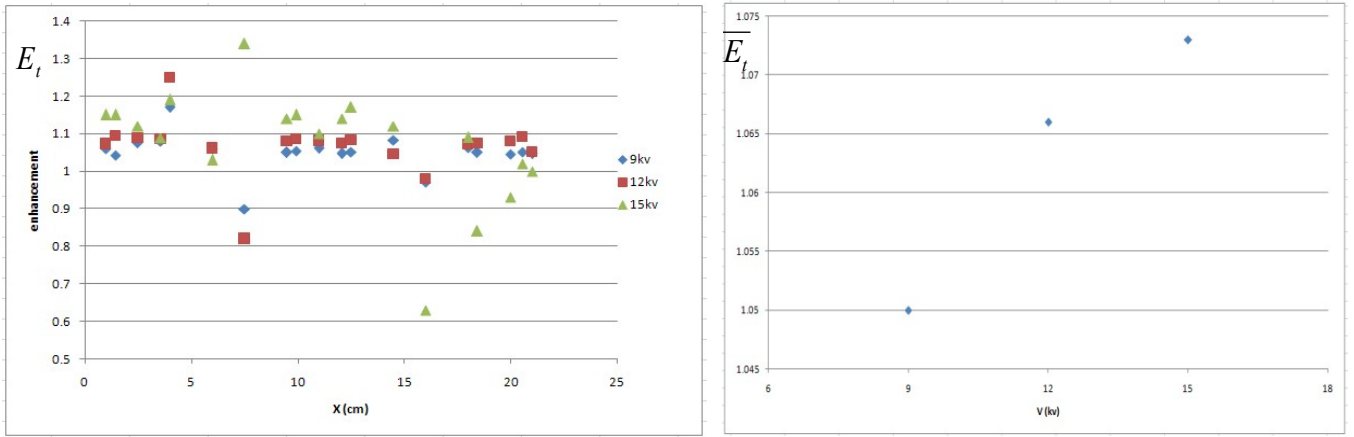


Fig. 8. Comparison of local and average rate of heat transfer enhancement on rib's surface direction for arrangement 1 and  $Re_{D_h} = 0$

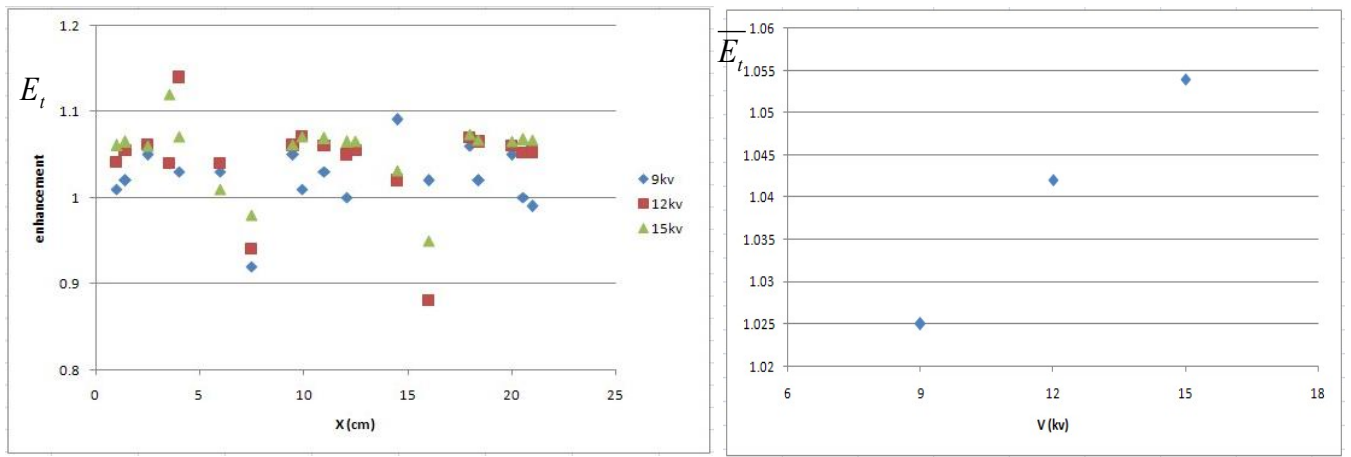


Fig. 9. Comparison of local and average rate of heat transfer enhancement on rib's surface direction for arrangement 2 and  $Re_{D_h} = 0$

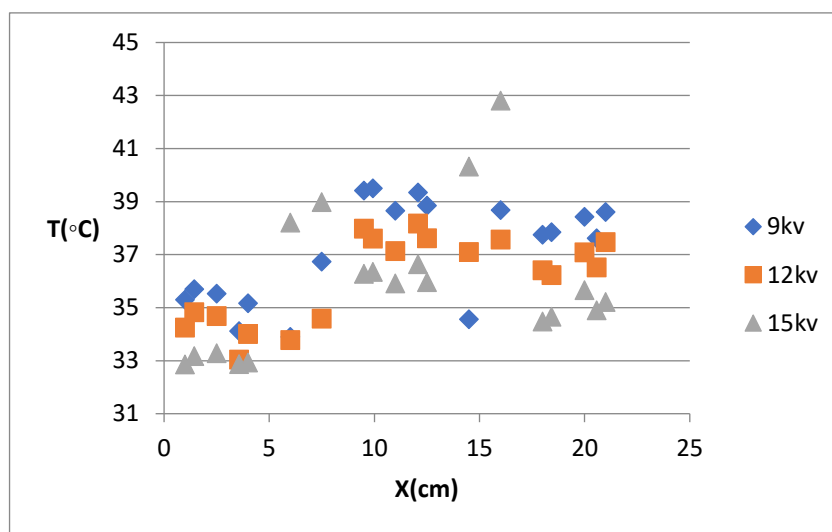


Fig. 10. Wall temperature distribution on rib's surface direction for arrangement 1 and  $Re_{D_h} = 500$

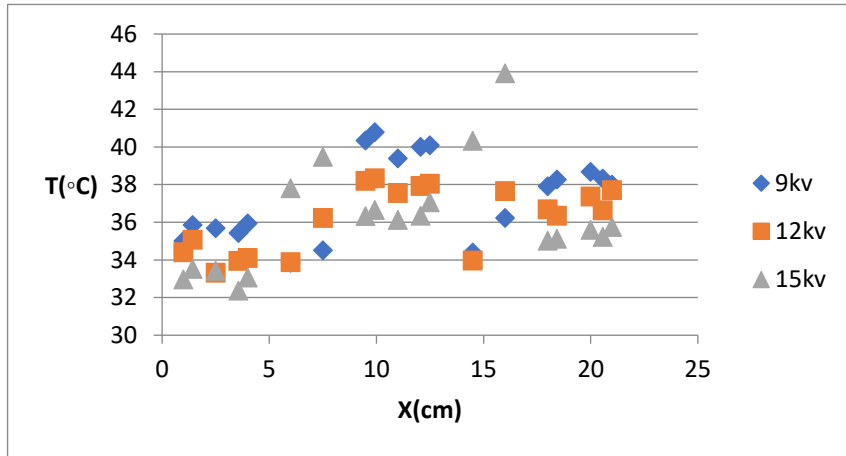


Fig. 11. Wall temperature distribution on rib's surface direction for arrangement 2 and  $Re_{D_h} = 500$

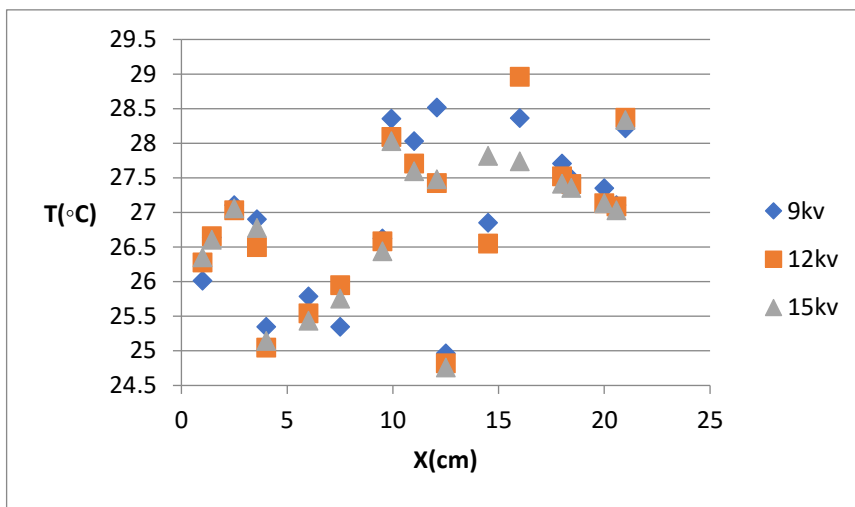


Fig. 12. Wall temperature distribution on rib's surface direction for arrangement 1 and  $Re_{D_h} = 4500$

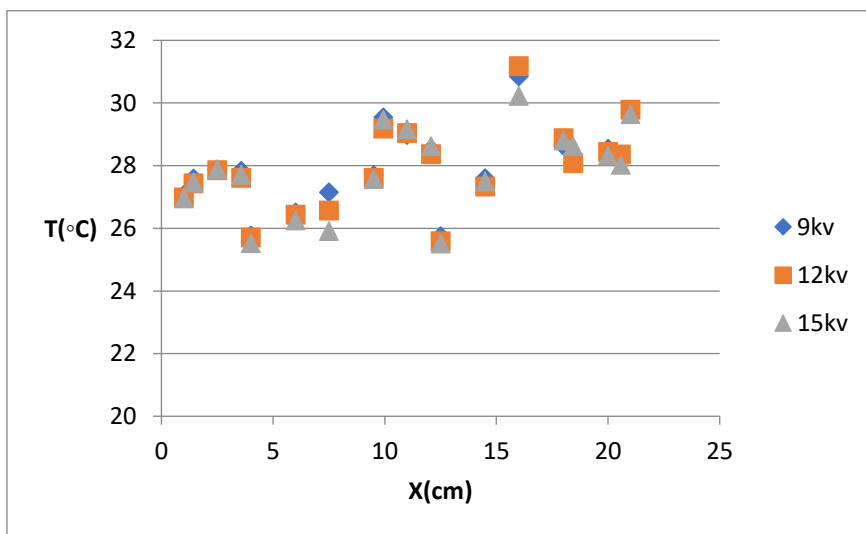


Fig. 13. Wall temperature distribution on rib's surface direction for arrangement 2 and  $Re_{D_h} = 4500$

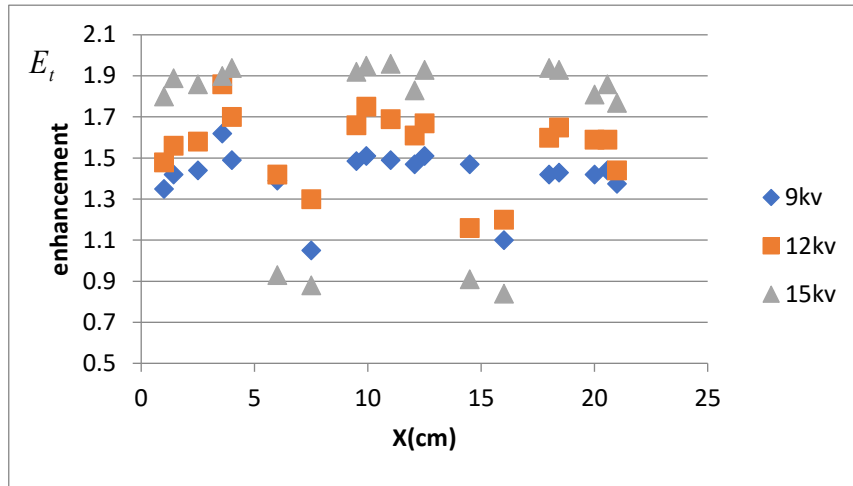


Fig. 14. Local rate of heat transfer enhancement on rib's surface direction for arrangement 1 and  $Re_{D_h} = 500$  (9, 12 and 15 kV)

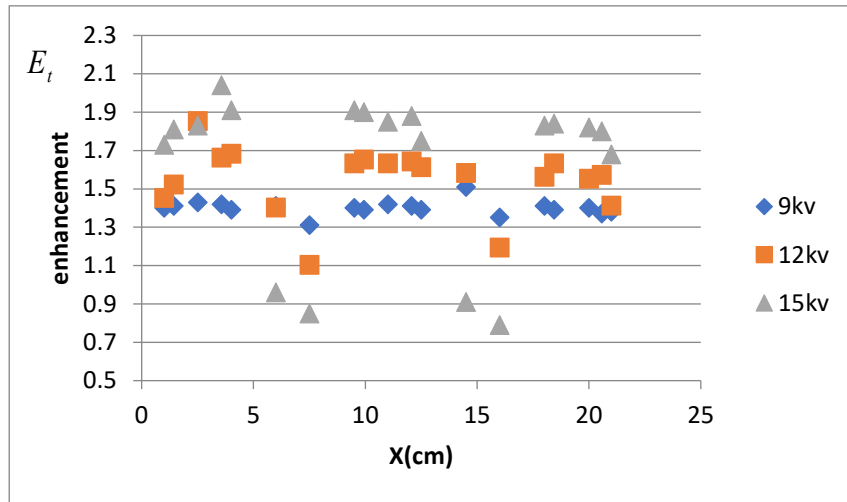


Fig. 15. Local rate of heat transfer enhancement on rib's surface direction for arrangement 2 and  $Re_{D_h} = 500$  (9, 12 and 15 kV)

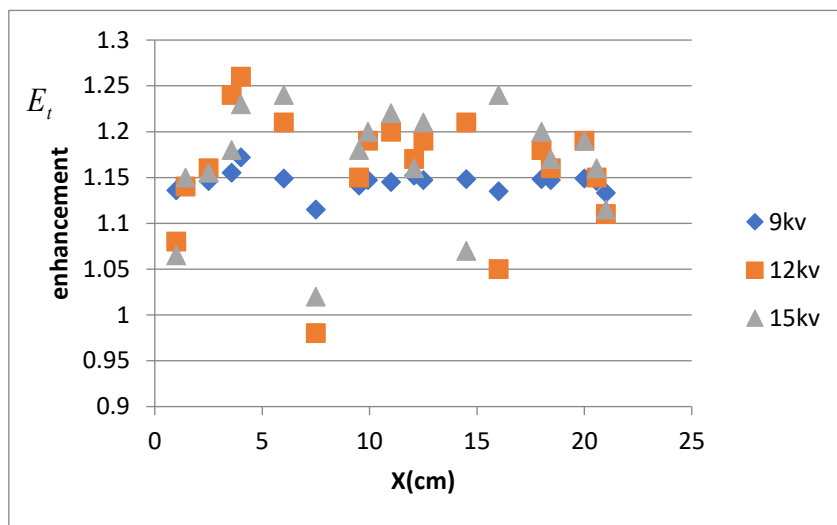


Fig. 16. Local rate of heat transfer enhancement on rib's surface direction for arrangement 1 and  $Re_{D_h} = 4500$  (9, 12 and 15 kV)

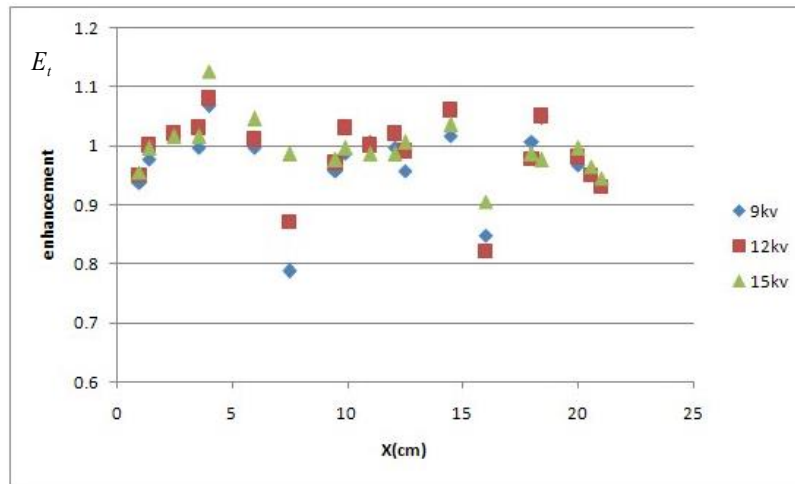


Fig. 17. Local rate of heat transfer enhancement on rib's surface direction for arrangement 2 and  $Re_{D_h} = 4500$  (9, 12 and 15 kV)

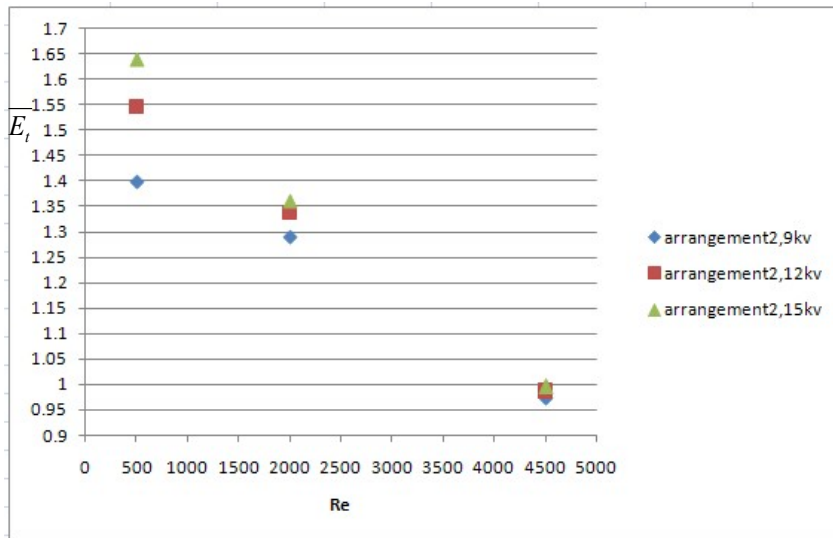


Fig. 18. Comparison of the average rate of heat transfer enhancement with arrangement 1 for 9, 12 and 15kV

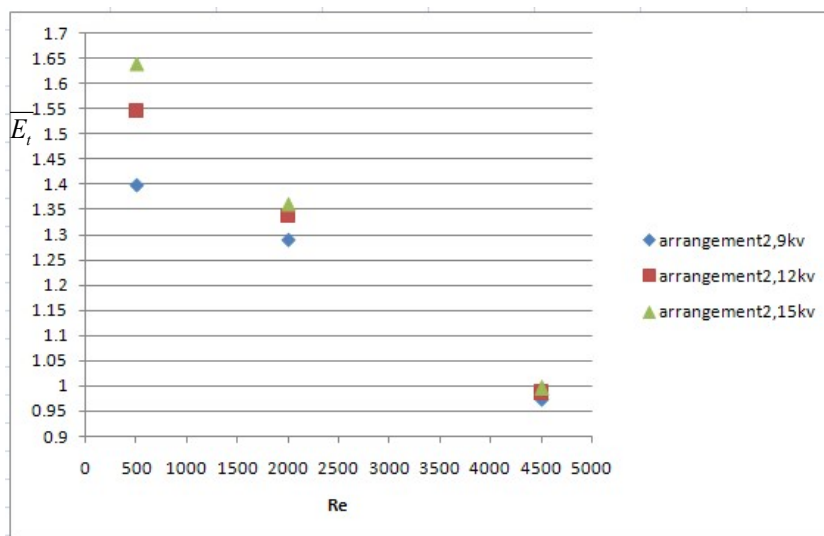


Fig. 19. Comparison of the average rate of heat transfer enhancement with arrangement 2 for 9, 12 and 15kV

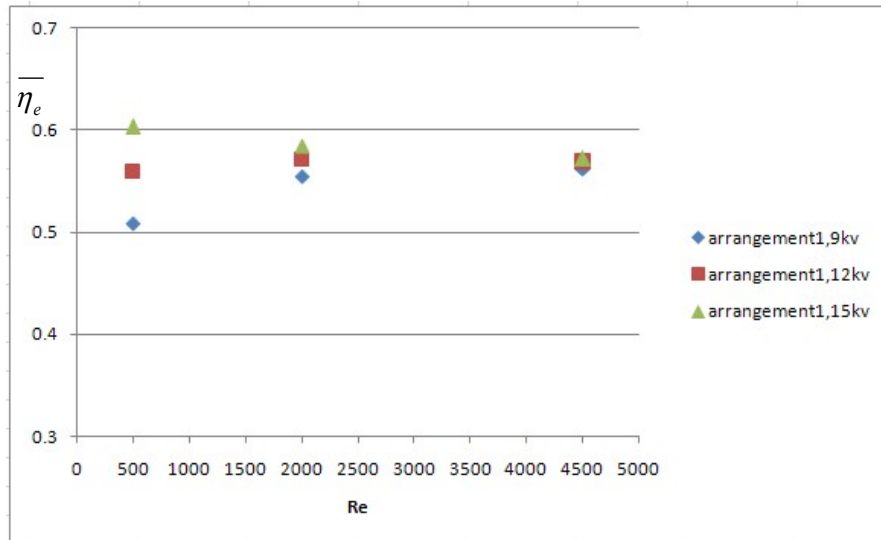


Fig. 20. The average performance evaluation criteria with arrangement 1 for 9, 12 and 15kV

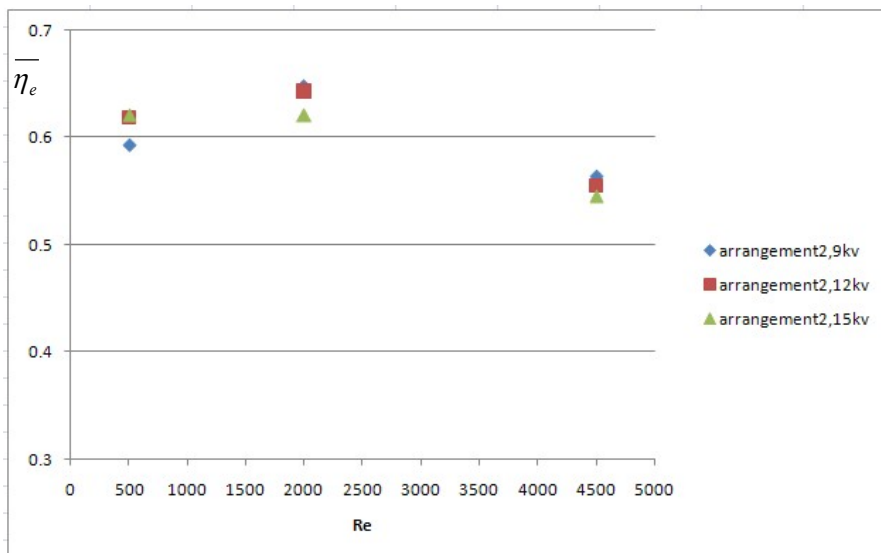


Fig. 21. The average performance evaluation criteria with arrangement 2 for 9, 12 and 15kV

(secondary flow) in the main flow eliminating the effects of corona wind.

The power of corona wind in a low Reynolds number is higher than that in a high Reynolds number. Therefore, the corona wind in laminar flows affects the main flow better than in situations of turbulent flows.

As it is seen in Figs. 18 and 19, comparison of the average rate of heat transfer enhancement is shown. With attention to these Figures, arrangement 1 is better than arrangement 2.

In Figs. 20 and 21, the variations of  $\bar{\eta}_e$  in  $Re_{D_0} = 500, 2000$  and  $4500$  have been shown. The effect of Reynolds number on heat transfer enhancement for active method shows the opposite behavior for both laminar and turbulent flows. With attention to these Figures, the pressure loss around of wire electrode in arrangement 1 is higher than that in arrangement 2. As a consequence, arrangement 2 is better than arrangement 1. Also, effect of flow in  $Re_{D_0} = 2000$  for

positive interaction of the average heat transfer enhancement and consumed power ratio seems to be better than other Reynolds numbers.

The uncertainty analysis for  $E_t, \eta_e, \bar{E}_t$  and  $\bar{\eta}_e$  has been achieved. The uncertainty for local quantities of  $E_t$  and  $\eta_e$  is smaller than 8% and for average quantities of  $\bar{E}_t$  and  $\bar{\eta}_e$  is 3.34% and 4.5% respectively [14]. In Figs. 22 and 23, the uncertainty analysis for various temperatures and  $E_t$  points obtained from one sample of iterative tests is presented. In Table 1, the values of uncertainty analysis with error calculation have been reported.

#### 4- Conclusions

The active method for low Reynolds numbers with laminar flows is advantageous. The average and local heat transfer enhancement climb up to 167.6% and 205%, respectively.

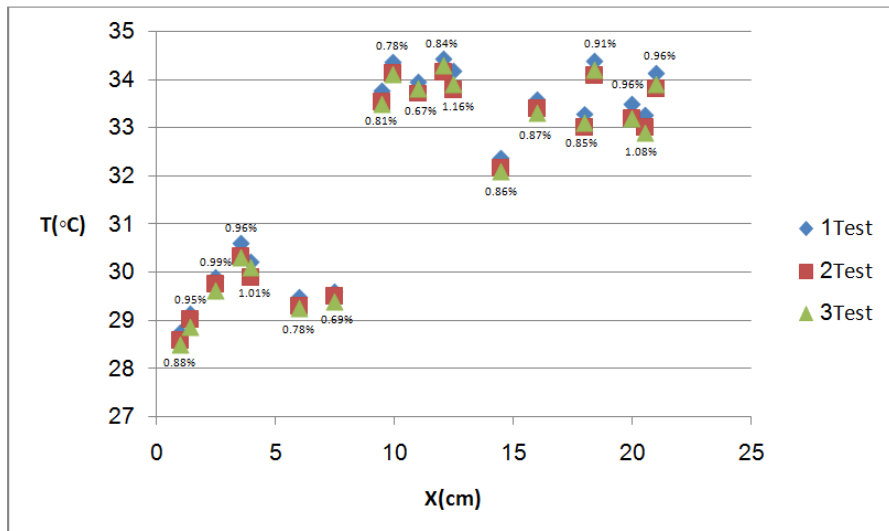


Fig. 22. Uncertainty analysis in various temperature points

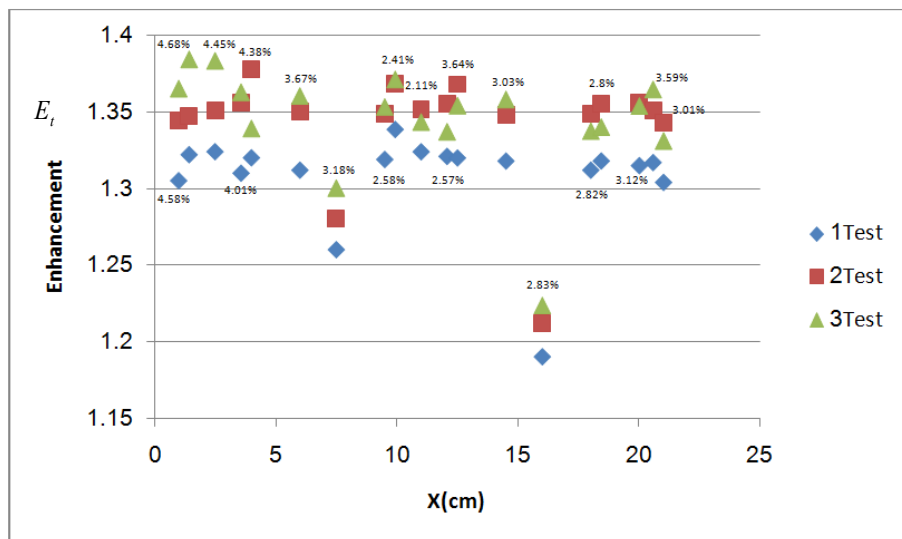


Fig. 23. Uncertainty analysis in various  $E_t$  points

Table 1. Average uncertainty analysis of all measured parameters

	$P$ (Pressure)	$V$ (Velocity)	$T$ (Temperature)	$\bar{E}_t$	$\bar{\eta}_e$
%Error	3	2.75	1	3.34	4.5

Active method for low Reynolds numbers has higher average performance evaluation criteria equal to 0.647. The power of corona wind in low Reynolds number is higher than high Reynolds number. Therefore, the corona wind in laminar flows has been affected on heat transfer enhancement better than turbulent flows.

For the same Reynolds numbers and wire arrangements, the heat transfer enhancement was increased with increments

in voltage of the wire electrodes. At high voltages, the density of electric charge around wire electrode in arrangement 1 is higher than that in arrangement 2. As a consequence, arrangement 1 is better than arrangement 2. Also, the corona wind in high voltages has been affected on heat transfer enhancement better than low voltages.

The power of corona wind in low Reynolds number flows is higher than in high Reynolds number flows, signifying that

the corona wind in laminar flows is better than in turbulent flows.

In the same Reynolds numbers and voltages of wires, the average performance evaluation criteria were increased in arrangement 2 than arrangement 1.

## NOMENCLATURE

b:	Mobility of ions [ $\text{m}^2 \cdot \text{V}^{-1} \cdot \text{s}^{-1}$ ]
C:	Distance between wire and ground electrodes [m]
D:	Diameter of pipe [m]
d:	Diameter of Orifice [m]
$D_h$ :	Hydraulic diameter [m]
$E_t$ :	Heat transfer enhancement ratio
$E_{lost}$ :	Consumed power ratio
$E_0$ :	Electric field [ $\text{V} \cdot \text{m}^{-1}$ ]
H:	Channel height [m]
h:	Heat transfer coefficient [ $\text{W} \cdot \text{m}^{-2} \cdot \text{K}^{-1}$ ]
$h_s$ :	Heat transfer coefficient for plain case
$I_0$ :	Electric current of corona wind [A]
L:	Width of trapezoidal rib [m], characteristic length [m]
$L_1$ :	Length of upstream region [m]
$L_2$ :	Length of downstream region [m]
M:	Mach number
$N_{EHD}$ :	EHD number
P:	Pressure [Pa]
$q_{rib}''$ :	Constant heat flux from trapezoidal rib [ $\text{W} \cdot \text{m}^{-2}$ ]
$q_{e0}$ :	Electric charge of one electron [Coulomb]
Re:	Reynolds number
$Re_{D_h}$ :	Reynolds number based on hydraulic diameter ( $v D_h / \nu$ )
r:	Radius of wire electrode [m]
$r_{eff}$ :	Effective radius of wire to ground electrode [m]
S:	Separation between trapezoidal ribs [m]
T:	Temperature [K, °C]
$u_i$ :	Velocity of electric ions [ $\text{m} \cdot \text{s}^{-1}$ ]
v:	Velocity [ $\text{m} \cdot \text{s}^{-1}$ ]
W:	Width of channel [m]
x,y,z:	Cartesian coordinates

## Greek symbols

$\alpha$ :	View angle between wire and ground electrodes
$\beta$ :	The ratio in diameter (orifice to pipe)
$\eta_e$ :	Performance evaluation criteria (PEC)
$\nu$ :	Kinematics viscosity [ $\text{m}^2 \cdot \text{s}^{-1}$ ]
$\rho_f$ :	Density of fluid [ $\text{kg} \cdot \text{m}^{-3}$ ]
$\rho_e$ :	Density of electric charge [ $\text{kg} \cdot \text{m}^{-3}$ ]
$\Delta$ :	Difference

## Subscripts

e:	Electron
----	----------

f:	Fluid
i:	Ions
ref.:	Reference condition
s:	plain case
T:	Constantan
t:	Enhancement
w:	Trapezoidal rib wall

## Superscripts

“:	Flux
-:	Avera

## REFERENCES

- [1] A. Alamgholilou (Alami nia), E. Esmaeilzadeh, Experimental Investigation on Hydrodynamics and Heat Transfer of Fluid Flow into Channel for Cooling of Rectangular Ribs by Passive and EHD Active Enhancement Methods, *Experimental Thermal and Fluid Science*, 38 (2012) 61-73.
- [2] A. Alamgholilou (Alami nia), E. Esmaeilzadeh, Numerical Investigation on Effects of Secondary Flow into Duct for Cooling of the Ribs by Passive Enhancement Method, *Enhanced Heat Transfer* 19(3) (2008) 233-248.
- [3] E. Esmaeilzadeh, A. Alamgholilou (Alami nia), Numerical Investigation of Heat Transfer Enhancement of Rectangular Ribs with Constant Heat Flux located in the floor of a 3D duct flow, *Asian Journal of Applied Sciences*, 1(4) (2008) 286-303.
- [4] A. Alami nia, A. Campo, Experimental Investigation on Flow and Heat Transfer for Cooling Flush-Mounted Ribbons in a Channel-Application of an Electrohydrodynamics Active Enhancement Method, *Thermal Science*, 20(2) (2016) 505-516.
- [5] A. Alami nia, A. Campo, Experimental study on EHD heat transfer enhancement from flush-mounted ribbons with different arrangements of wire electrodes in a channel, *Heat Mass Transfer*, 52 (2016) 2823-2831.
- [6] A. Alami nia, T. Kheiri, M. Jafari, Experimental Study on Electrohydrodynamic Heat Transfer Enhancement of Semicircular Ribs into Channel, *Thermal Science*, 23(2A) (2019) 497-508.
- [7] M. Peng, T.H. Wang, X.D. Wang, Effect of longitudinal electrode arrangement on EHD-induced heat transfer enhancement in a rectangular channel, *International Journal of Heat and Mass Transfer*, 93 (2016) 1072-1081.
- [8] W. J. Sheu, J.J. Hsiao, C.C. Wang, Effect of oscillatory EHD on the heat transfer performance of a flat plate, *International Journal of Heat and Mass Transfer*, 61 (2013) 419-424.
- [9] H. M. Deylami, N. Amanifard, F. Dolati, R. Kouhikamali, K. Mostajiri, Numerical investigation of using various electrode arrangements for amplifying the EHD enhanced heat transfer in a smooth channel, *Journal of Electrostatics*, 71 (2013) 656-665.
- [10] H. Fujishima, Y. Morita, M. Okubo, T. Yamamoto, Numerical Simulation of Three-dimensional EHD of Spiked-Electrode Electrostatic Precipitators, *IEEE*, 13(1) (2006) 160-167.
- [11] M. M. Ohadi, D.A. Nelson, S. Zia, Heat Transfer Enhancement of Laminar and Turbulent Pipe Flow via Corona Discharge, *Int. Journal of Heat and Mass Transfer*, 34 (1991) 1175-1187.
- [12] N. F. Homologuee, *Mesure De Debit Des Fluids Au Moyen De Diaphragms*, NF X 10-102, (1971).
- [13] J. H. Goo, J.W. Le, Stochastic Simulation of Particle Charging and Collection Characteristics for Wire-Plate Electrostatic Precipitator of Short Length, *Aerosol Science*, 28(5) (1997) 875-893.
- [14] R. J. Moffat, Describing the Uncertainties in Exp. Results, *Exp. Thermal & Fluid Science*, 1 (1988) 3-17.

### HOW TO CITE THIS ARTICLE

A. Alami-nia. *Experimental Investigation on Effects of Trapezoidal Ribs on Heat Transfer Enhancement with Electrohydrodynamics Active Method into Duct*. *AUT J. Mech Eng.*, 4(4): (2020) 493-504.

DOI: 10.22060/ajme.2020.16725.5840

